



**HAL**  
open science

## **Baseline circulating tumour DNA and total metabolic tumour volume as early outcome predictors in aggressive large B-cell lymphoma. A real-world 112-patient cohort**

Enora Le Goff, Paul Blanc-durand, Louise Roulin, Charlotte Lafont, Romain Loyaux, Diana-laure Mboumbae, Ichrafe Benmaad, Alexis Claudel, Elsa Poullot, Cyrielle Robe, et al.

### ► To cite this version:

Enora Le Goff, Paul Blanc-durand, Louise Roulin, Charlotte Lafont, Romain Loyaux, et al.. Baseline circulating tumour DNA and total metabolic tumour volume as early outcome predictors in aggressive large B-cell lymphoma. A real-world 112-patient cohort. *British Journal of Haematology*, 2023, 10.1111/bjh.18809 . hal-04134838

**HAL Id: hal-04134838**

**<https://hal.u-pec.fr/hal-04134838>**



Submitted on 20 Jun 2023

**HAL** is a multi-disciplinary open access archive for the deposit and dissemination of scientific research documents, whether they are published or not. The documents may come from teaching and research institutions in France or abroad, or from public or private research centers.

L'archive ouverte pluridisciplinaire **HAL**, est destinée au dépôt et à la diffusion de documents scientifiques de niveau recherche, publiés ou non, émanant des établissements d'enseignement et de recherche français ou étrangers, des laboratoires publics ou privés.

## ORIGINAL PAPER

# Baseline circulating tumour DNA and total metabolic tumour volume as early outcome predictors in aggressive large B-cell lymphoma. A real-world 112-patient cohort

Enora Le Goff<sup>1</sup>  | Paul Blanc-Durand<sup>2,3</sup> | Louise Roulin<sup>1</sup> | Charlotte Lafont<sup>3,4</sup> | Romain Loyaux<sup>5</sup> | Diana-Laure MBoumbae<sup>3,5</sup> | Ichrafe Benmaad<sup>5</sup> | Alexis Claudel<sup>5</sup> | Elsa Pouillot<sup>6</sup> | Cyrielle Robe<sup>6</sup> | Guillaume Gricourt<sup>7</sup> | Abdelrazak Aissat<sup>7</sup> | Christiane Copie-Bergman<sup>3,6</sup> | François Lemonnier<sup>1,3</sup> | Philippe Gaulard<sup>3,6</sup> | Emmanuel Itti<sup>2,3</sup> | Corinne Haioun<sup>1,3</sup> | Marie-Helene Delfau-Larue<sup>3,5</sup> 

<sup>1</sup>Lymphoid Malignancies Unit, Assistance Publique des Hôpitaux de Paris, HU Henri Mondor, Créteil, France

<sup>2</sup>Nuclear Medicine Department, Assistance Publique des Hôpitaux de Paris, HU Henri Mondor, Créteil, France

<sup>3</sup>Paris-Est Créteil University, INSERM, IMRB, F-94010, Créteil, France

<sup>4</sup>Public Health Department, Assistance Publique des Hôpitaux de Paris, HU Henri Mondor, Créteil, France

<sup>5</sup>Hematobiology and Immunobiology Department, Assistance Publique des Hôpitaux de Paris, HU Henri Mondor, Créteil, France

<sup>6</sup>Pathology Department, Assistance Publique des Hôpitaux de Paris, HU Henri Mondor, Créteil, France

<sup>7</sup>Bioinformatics Department, Assistance Publique des Hôpitaux de Paris, HU Henri Mondor, Créteil, France

## Correspondence

Marie-Helene Delfau-Larue, Hematologic and Immunologic Biology Department, Assistance Publique Hôpitaux de Paris, GH Mondor, 51 avenue du Maréchal Delattre de Tassigny, 94000 Créteil, France.  
 Email: [marie-helene.delfau@hmn.aphp.fr](mailto:marie-helene.delfau@hmn.aphp.fr)

## Summary

Approximately 20%–50% of patients with large B-cell lymphoma (LBCL) experience poor outcomes. We aimed to evaluate the combined prognostic value of circulating tumour DNA (ctDNA) and total metabolic tumour volume (TMTV) in LBCL. This observational single-centre study included 112 newly diagnosed LBCL patients, receiving R-CHOP/R-CHOP-like chemotherapies. CtDNA load was calculated following next-generation sequencing of cell-free DNA (cfDNA) using a targeted 40-gene lymphopanel. TMTV was measured using a fully automated artificial intelligence-based method for lymphoma lesion segmentation. CtDNA was detected in cfDNA samples from 95 patients with a median concentration of 3.15 log haploid genome equivalents per mL. TMTV measurements were available for 102 patients. The median TMTV was 501 mL. High ctDNA load (>3.57 log hGE/mL) or high TMTV (>200 mL) were associated with shorter 1-year PFS (44% vs. 83%,  $p < 0.001$  and 64% vs. 97%,  $p = 0.002$ , respectively). When combined, three prognostic groups were identified. The shortest PFS was observed when both TMTV and ctDNA load were high ( $p < 0.001$ ). Even with a short follow up, combining ctDNA load with TMTV improved the risk stratification of patients with aggressive LBCL. In the near future, very high-risk patients could benefit from CAR T-cell therapy or bispecific antibodies as first-line treatments.

## KEY WORDS

circulating tumour DNA, non-Hodgkin lymphoma, neoplasm staging, positron emission tomography computed tomography, prognosis

## INTRODUCTION

Aggressive large B-cell lymphoma (LBCL) including diffuse large B-cell lymphoma (DLBCL), high grade B-cell lymphoma (HGBL) and primary mediastinal B-cell lymphoma (PMBL)

are the most common subtypes of non-Hodgkin lymphoma.<sup>1,2</sup> The addition of rituximab to cyclophosphamide-doxorubicin-vincristine-prednisone (R-CHOP) chemotherapy has greatly improved the outcome of LBCL patients.<sup>3</sup> However, approximately 20%–50% still experience a poor outcome.<sup>4,5</sup>

The authors thank Emma Pilling for language editing services and Marielle Romet (Sante Active Edition) for general editing services.

This is an open access article under the terms of the [Creative Commons Attribution-NonCommercial-NoDerivs](https://creativecommons.org/licenses/by-nc-nd/4.0/) License, which permits use and distribution in any medium, provided the original work is properly cited, the use is non-commercial and no modifications or adaptations are made.

© 2023 The Authors. *British Journal of Haematology* published by British Society for Haematology and John Wiley & Sons Ltd.

Several scores have been developed to improve their prognostic stratification. The International Prognostic Index (IPI) remains the most widely used tool for assessing patient prognosis in routine clinical practice.<sup>6–9</sup> Other prognostic factors have been identified like gene expression profiling<sup>10–16</sup> or HGBL subtype.<sup>1,2,17–20</sup> However, these clinical and pathological features are not sufficient to reflect the full LBCL heterogeneity.

Imaging by <sup>18</sup>F-fluorodeoxyglucose-positron emission tomography/computed tomography (FDG-PET/CT) is now recommended for the initial evaluation and response assessments of aggressive lymphoma.<sup>21–23</sup> The total metabolic tumour volume (TMTV) is obtained by summing the metabolic volumes of all the nodal and extranodal lesions and seems to provide a good reflection of tumour burden at diagnosis.<sup>22,24</sup> A high TMTV at diagnosis has been reported to be associated with a poorer outcome.<sup>15,25,26</sup>

Circulating tumour DNA (ctDNA) is a new biological parameter not yet widely used in clinical practice. CtDNA is being increasingly studied as a potential new strategy for lymphoma profiling and patient management. Circulating cell-free DNA (cfDNA) refers to extracellular DNA fragments present in the body fluid. Higher concentrations have been observed in cancer patients due to the presence of ctDNA derived from tumour cells undergoing apoptosis.<sup>27</sup> Next-generation sequencing (NGS) and advances in PCR have enabled the detection of somatic variants in ctDNA. Panels of target genes have been validated for lymphoma<sup>10,28,29</sup> allowing the molecular characterization of LBCL in the plasma, as well as in tumour biopsies. It has been suggested that ctDNA analysis would provide a better reflection of the genetic heterogeneity of LBCL than the analysis of the tissue biopsy itself.<sup>27,28,30</sup> Some studies have also reported that a high ctDNA load at diagnosis may be associated with a poorer prognosis.<sup>29–35</sup>

The goal of this study was to evaluate the real-world prognostic value of TMTV and cfDNA, both individually and in combination, in a cohort of patients with newly diagnosed aggressive LBCL.

## METHODS

### Study design and patients

This observational single-center study was conducted on patients attending the Lymphoma Unit, Créteil University Hospital, APHP, France and included during two periods. From May 2017 to March 2019, cfDNA was analysed from plasma prospectively collected in EDTA tubes from patients participating in the RT3 trial (Real Time Molecular Characterization of Diffuse Large B Cell Lymphoma trial)<sup>36</sup> with sufficient tumoral material available for NGS analyses. From March 2019 to December 2020, cfDNA was analysed from plasma samples collected in Streck tubes from all newly diagnosed patients, regardless of the amount of tumoral material available. The date of the last follow up was 3 July

2021. All patients provided written informed consent before being included in the analysis for the current study, in accordance with both institutional ethical guidelines and the Declaration of Helsinki. The local institutional review board (CPP number 15071, ANSM IDRCB2015-A00342-47) approved the retrospective collection and analysis of the data.

Patients meeting the following inclusion criteria were included: (i) aged  $\geq 18$  years, (ii) untreated LBCL, diagnosed as DLBCL-not otherwise specified (NOS), HGBL double hit (HGBL-DH), triple hit (HGBL-TH) or NOS (HGBL-NOS) and as PMBL, according to the criteria of the 2016 WHO classification,<sup>2</sup> (iii) eligible for first-line treatment with a combination of anthracycline-based chemotherapy and an anti-CD20 monoclonal antibody and (iv) with blood samples for cfDNA analysis collected at diagnosis. Patients with untreated transformed low-grade NHL and those with positive HIV serology were eligible. Patients with diagnoses of Burkitt lymphoma, follicular lymphoma grade IIB, primitive cerebral lymphoma or plasmablastic lymphoma, as well as those eligible for immunotherapy alone, were excluded.

Data on clinical features at diagnosis and treatment regimens were retrospectively collected from hospital records. Data concerning responses to treatment and the date of first event (relapse, progression, death of any cause), were collected during follow up.

### Sample collection and cfDNA sequencing

For all patients, blood samples were collected at baseline before any treatment. Plasma (2–4 mL) was isolated within 4 h and frozen at  $-20^{\circ}\text{C}$ . DNA extraction was performed using a QIA Symphony automated extraction device (Qiagen). DNA samples were then stored at  $-20^{\circ}\text{C}$  until analysis (Research collection, Assistance Publique Hôpitaux de Paris).

Quantification of cfDNA was carried out by droplet digital PCR (ddPCR) assay using the QX200 Droplet Digital PCR system (Bio-Rad Laboratories), as previously described.<sup>37</sup> The quantity of cfDNA in plasma was expressed as the haploid genome equivalents per mL of plasma (log hGE/mL).

Sequencing libraries were prepared using the QIAseq library kit (QIAGEN) according to the manufacturer's instructions. Briefly, 10–40 ng of cfDNA were end-repaired, A-tailed, and ligated to UMI (Unique molecular identifier) barcoded adapters. The adapter-ligated libraries were target enriched by PCR (6 cycles) using a panel of loci-specific primers targeting a lymphopanel of 40 targeted genes (Table S1). The target-enriched libraries were then further amplified with 21 cycles of PCR. The library profile was analysed using the Agilent 2100 Bioanalyzer (Agilent Technologies) and quantified by qPCR using the QIAseq Library Quant Assay Kit (QIAGEN). For each single sequencing run, a multiplexed (8-plex) library was created by pooling libraries at an equal molar ratio, as determined by qPCR. The multiplexed library was denatured and sequenced using the Illumina MiSeq kit (2  $\times$  150 cycles with pair-end runs). Bioinformatic analysis was performed using the QIAseq open sources analysis pipeline.

The mean variant allele frequency (VAF) was calculated for non-synonymous coding variants by dividing by 2 the VAF of variants for which the deletion of the corresponding normal allele could be visualized by the loss of a known polymorphism and/or confirmed by biopsy analysis. Concentrations of ctDNA were expressed in log hGE/mL, calculated by multiplying the mean VAF by the concentration of cfDNA.

## <sup>18</sup>F-Fluorodeoxyglucose-positron emission tomography/computed tomography

All patients underwent <sup>18</sup>F-fluorodeoxyglucose-positron emission tomography/computed tomography (FDG-PET/CT) in the nuclear medicine department at the following times during the study period: at diagnosis for initial staging, mid-treatment depending on the treatment strategy, and at the end of treatment or in case of suspected relapse or progression. Disease response was assessed by FDG-PET/CT in accordance with the Lugano Classification<sup>23</sup> and using the Deauville five-point scale.<sup>38</sup>

FDG-PET/CT scans were performed 60 minutes after injection of FDG, either on a Gemini GXL16 scanner (Philips) or on a Biograph Vision 450 scanner (Siemens). Quality control of image reconstruction was ensured by measuring the SUVmax in a spherical volume of interest (VOI) in the liver and in the mediastinum. Image volumes were imported in a DICOM format onto an Imagys workstation (Keosys). Lymphoma lesions were identified visually as areas of increased uptake outside areas of physiological uptake. The CT fusion display was used to ensure that the metabolic volumes did not spill over into anatomical structures. The TMTV was obtained by summing the metabolic volumes of all individual nodal and extranodal lesions, using a semi-automated artificial-intelligence-based tool for the segmentation of lymphoma lesions using the PAIRE software v1.0.0.<sup>39</sup>

## Pathology

The diagnosis was made by expert hematopathologists belonging to the French Lymphopath network, according to the criteria of the 2016 WHO classification.<sup>2</sup> Immunohistochemistry was performed using a panel of antibodies comprising at least those directed against CD20, CD5, CD10, BCL-6, MUM-1, Ki67, BCL-2 and MYC allowing for the determination of the cell-of-origin status of the DLBCL according to the Hans algorithm.<sup>40</sup>

Analysis of *BCL6*, *MYC* and *BCL2* rearrangements was done by fluorescence in situ hybridization (FISH) as previously described<sup>20</sup> to identify patients with HGBL-DH (*MYC* and *BCL2* or *BCL6* rearrangements) or HGBL-TH (*MYC*, *BCL2* and *BCL6* rearrangements).

When available, tumour tissue samples were also sequenced by NGS. Tumour sequencing was conducted in the

pathology department (Henri Mondor University Hospital), according to the method described by Bohers et al.<sup>41</sup> using a 36-gene lymphopanel (Table S1, sheet 1) and amplicon-based libraries on an Ion Torrent Personal Genome machine (Thermo Fisher Scientific). All the genes included in the 36-gene lymphopanel were also included in the 40-gene cfDNA lymphopanel.

## Statistical analysis

Receiver-operating characteristic (ROC) and X-tile analysis<sup>42</sup> analysis were performed to determine optimal cut-off values for survival predictions. Briefly, a ROC analysis was performed to determine the optimal cut-off value for each continuous variable (ctDNA and TMTV) for stratifying the population according to binary progression-free survival (PFS) patient status (0 = no progression vs. 1 = progression) and for achieving the best compromise between sensitivity and specificity (Youden index = Se + Sp - 1). The X-tile software<sup>40</sup> was then used for biomarker assessment and outcome-based cut-off optimization, and Kaplan–Meier analyses of survival were performed for each continuous variable (ctDNA and TMTV), taking into account the time of progression and time of censoring, in addition to the binary classification of PFS.

Patient characteristics according to ctDNA group were compared using the chi-squared or Fisher exact tests for categorical variables, as appropriate, and the Student's *t* test for continuous variables after assessing the normality of the distribution.

PFS was measured from the date of diagnosis to the date of progression, relapse, death from any cause, or last follow up (censored data). Overall survival (OS) was measured from the date of diagnosis to the date of death from any cause or last follow up (censored data). Survival rates were expressed as percentages with 95% confidence intervals (CIs). Kaplan–Meier survival curves were compared using the log-rank test. The proportional hazards assumption was verified. Uni- and multivariable analyses were performed using Cox proportional hazards models. Variables associated with a  $p < 0.2$  or deemed clinically relevant were selected as candidates for the multivariable Cox model for PFS. The final model was reached using a backward selection procedure, leading to elimination of the non-significant variables with the highest *p*-values ( $>0.05$ ) only when this elimination did not lead to a significant change in the coefficient and/or *p*-value of the other variables in the model. As less than 40 events were observed in our cohort, the number of variables included in the multivariate analysis was limited. Interactions were tested and hazard ratios (HRs) with 95% CIs were calculated.

Statistical significance was defined as a  $p < 0.05$ . Statistical analyses were conducted using the X-tile 3.6.1 software (Yale University), MedCalc 12.2.1.0 (MedCalc Software) and the STATA 17 software (StataCorp 2021. Stata Statistical Software: Release 17.; StataCorp LLC.).

## RESULTS

### Clinical and histological features

Between May 2017 and December 2020, 112 untreated LBCL patients were included in the study (Figure 1). The clinical and demographic characteristics of the patients are listed in Table 1.

There were 87 DLBCL-NOS (78%); 17 HGBL<sup>15</sup>; 5 PMBL (4%); 2 T-cell-rich B-cell lymphoma (2%) and 1 intravascular DLBCL (1%). Transformed low-grade lymphoma was identified in 28 patients (25%). Median age was 67 years. Most of them presented an advanced disease: 93 (83%) had stage III or IV disease according to the Ann Arbor classification<sup>43</sup> and 61 (54%) had high IPI scores 3–5. Central nervous system (CNS) involvement was documented at diagnosis by flow cytometry in five patients.

### Treatments

Treatments are described in Table S2. Most patients received R-CHOP ( $n=83$ , 74%) or R-CHOP-like ( $n=11$ , 10%) chemotherapy. Seven patients (6%) with particularly aggressive disease (HGBL or CNS involvement at diagnosis), who were fit enough to meet the treatment criteria, received more intensive therapy following a Burkitt lymphoma treatment regimen.<sup>44</sup>

Patients considered as at high risk of CNS relapse (CNS-IPI score  $\geq 4$  or extranodal involvement, mostly in the testis) or treated with the intensive regimen, received CNS prophylaxis.

### Clinical outcomes

The median follow up was 17 months (range: 3–44 months). At last follow up, OS and PFS were 59% [95% CI: 26.9–81.3]

and 60% [95% CI: 46.6–70.4], respectively. The 1-year PFS was 73% [95% CI: 63.8–80.6] (Figure 2).

Nineteen patients (17%) presented disease progression during therapy, with a median time to progression of 3 months (range: 1–7 months). Complete and partial FDG-PET/CT metabolic responses after first-line treatment were observed in 88 (79%) and 5 (4%) patients, respectively. Relapse occurred in 17 patients (15%), with a median time to relapse of 9 months (range: 1–24 months). During follow up, 18 patients (16%) died: 12 from disease progression, one from hematologic toxicity and five from other causes not related to lymphoma (one from head and neck cancer, two from SARS-CoV-2 infection, one from sudden death likely due to cardiovascular or pulmonary embolism, and one after a fall and subsequent massive subdural hematoma). The median time to death was 10 months from diagnosis. At last follow up, five patients were still in progression and 89 were in complete metabolic response.

Significantly shorter PFS was observed in patients with HGBL ( $p<0.001$ ), bone marrow involvement ( $p=0.001$ ), IPI scores of 3–5 ( $p<0.001$ ) or CNS involvement ( $p=0.016$ ).

### FDG-PET/CT at diagnosis

TMTV data at diagnosis were available for 102 patients (the tumour was removed before FDG-PET/CT in four cases, urgent chemotherapy was required before FDG-PET/CT in three cases, data were uninterpretable in one case and the images could not be recovered in two cases).

The median baseline TMTV was 501 mL (range: 4–5151 mL).

A baseline TMTV threshold of 200 mL was selected and validated as the optimal cut-off for evaluating the correlation between baseline TMTV and PFS.

In univariate analysis, patients with a high TMTV at baseline ( $>200$  mL,  $n=69$ ) had significantly lower rates of 1-year

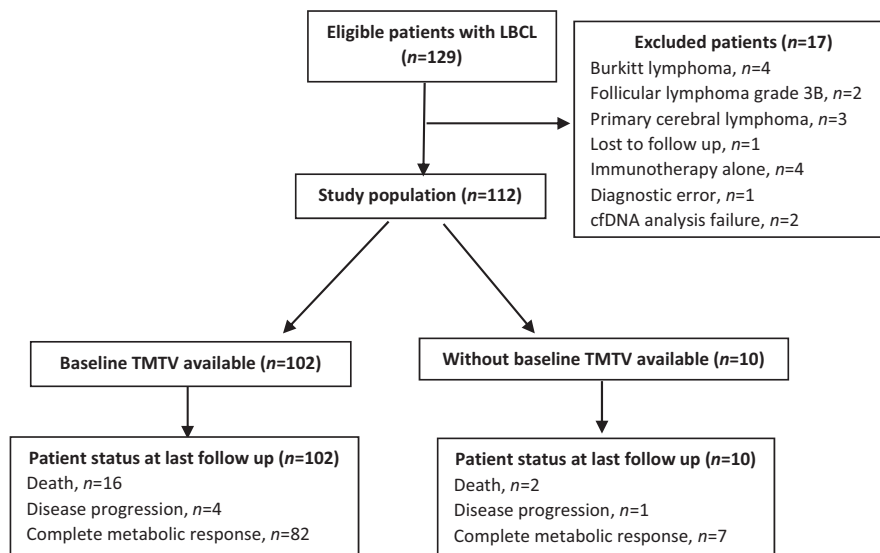


FIGURE 1 Flow chart of patient study inclusion.



**TABLE 1** Patient characteristics for the whole cohort.

Characteristics	Patients (n = 112)
Male sex, n (%)	68 (61)
Age (years), median [range]	67 [20–91]
Histological diagnosis, n (%)	
DLBCL	87 (78)
HGBL	17 (15)
PMBL	5 (4)
Other <sup>a</sup>	3 (3)
Transformed low grade, n (%)	28 (25)
Stage, n (%)	
I/II	19 (17)
III/IV	93 (83)
IPI, n (%)	
0–2	51 (46)
3–5	61 (54)
CNS-IPI, n (%)	
0–1	22 (20)
2–3	55 (49)
4–6	35 (31)
LDH level above normal, n (%)	67 (60)
Central nervous system localization <sup>b</sup> , n (%)	5 (4)
Bone marrow involvement <sup>c</sup> , n (%)	14 (13)
Histological features, n (%)	
GC	54 (48)
Non-GC	58 (52)
Double hit	11 (10)
Triple hit	2 (2)
Baseline circulating tumour DNA	
Detected, n (%)	95 (85)
Median [min-max], log hGE/mL	2.9 [0–5.0]
TP53 mutation <sup>d</sup> , n (%)	25 (26)
FDG-PET/CT <sup>e</sup>	
Baseline TMTV available, n (%)	102 (91)
Median [range] baseline TMTV, mL (n = 102)	501 [4–5151]
Median [range] baseline SUVmax (n = 102)	23.3 [4.6–54]

Abbreviations: CNS-IPI, Central Nervous system-International Prognostic Index (a score of 0–1 indicates low risk of CNS relapse, a score of 2–3 intermediate risk of CNS relapse and a score  $\geq 4$  points indicates high risk of CNS relapse); DLBCL, diffuse large B-cell lymphoma; FDG-PET/CT, <sup>18</sup>F-fluorodeoxyglucose-positron emission tomography/computed tomography; GC, germinal centre (according to Hans algorithm); HGBL, high grade B-cell lymphoma; IPI, International Prognostic Index (score of 0–2 indicate low to intermediate risk disease, score of 3–5 points indicate high-risk disease); LDH, lactate dehydrogenase level; PMBL, primary mediastinal large B-cell lymphoma; TMTV, total metabolic tumour volume.

<sup>a</sup>Two patients had T-cell-rich B-cell lymphoma and one had intravascular DLBCL.

<sup>b</sup>Data available for 109 patients.

<sup>c</sup>Data available for 105 patients.

<sup>d</sup>Among patients with ctDNA detected (n = 95).

<sup>e</sup>FDG-PET/CT data were available for 102 patients.

PFS than those with a TMTV < 200 mL at baseline (64% vs. 97%, respectively,  $p = 0.002$ , HR = 4.6 [95% CI: 1.6–13.2]) (Table 2 and Figure 3A). The same results were obtained when the analysis was restricted to patients who received R-CHOP-like treatment ( $p = 0.001$ , HR = 7.49 [95% CI: 3.47–16.17]). No interaction between the period of collection and TMTV prognostic value was found ( $p = 0.155$ ).

## Molecular characteristics

The mean coverage of the cfDNA samples was 518 UMI (range: 177×–1500×). At least one mutation was detected in 95 of 112 cases (85%; Table S1). The median number of non-synonymous coding variants per sample was 7 (range: 0–30) and the mean allele fraction was 16.9% (range: 1.2%–47%). The ctDNA genotyping results are presented in Figure 4. As expected, *TP53*, *PIM1* and *KMT2D* were the most frequently mutated genes. Tumour tissue samples from 77 patients were available for analysis (variants are detailed in Table S1). On average, 66% of the variants detected in ctDNA were present in the tumour (Table S1).

The ctDNA was quantified from the coding variants, with a median of 3.15 log hGE/mL (range: 1.4–5.0 log hGE/mL).

A ctDNA threshold of 3.57 log hGE/mL was selected and validated as the optimal cutoff for analysing the correlation between baseline ctDNA load and PFS. In univariate analysis, a significantly lower 1-year PFS was observed in patients with a high ctDNA load (>3.57 log hGE/mL,  $n = 28$ ) compared to those with a ctDNA load below the threshold: 44% vs. 83%, respectively;  $p < 0.001$ , HR = 3.1 [95% CI: 1.6–6.1] (Table 2 and Figure 3B). The same results were obtained when the analysis was restricted to patients who received R-CHOP-like treatment ( $p < 0.001$ , HR = 3.12 [95% CI: 1.31–7.42]). No interaction between the period of collection and ctDNA prognostic value was found ( $p = 0.448$ ).

Patients with a high ctDNA load presented more advanced disease at diagnosis with significantly more patients having stage III/IV disease ( $p = 0.039$ ), IPI scores of 3–5 ( $p < 0.001$ ) and above normal lactate dehydrogenase (LDH) levels ( $p < 0.001$ ) at diagnosis (Table 3).

Among the 95 patients with samples in which ctDNA was detected, 25 had a *TP53* mutation (26%) and had a shorter PFS ( $p = 0.004$ , HR = 2.63 [95% CI: 1.31–5.29]) (Figure 5).

## Combined prognostic value of ctDNA load at diagnosis and baseline TMTV

As expected, we found a significant relationship between ctDNA load at diagnosis and baseline TMTV ( $p < 0.001$ ). (Figure S1).

Combining baseline TMTV and ctDNA loads led to the identification of three groups with significantly

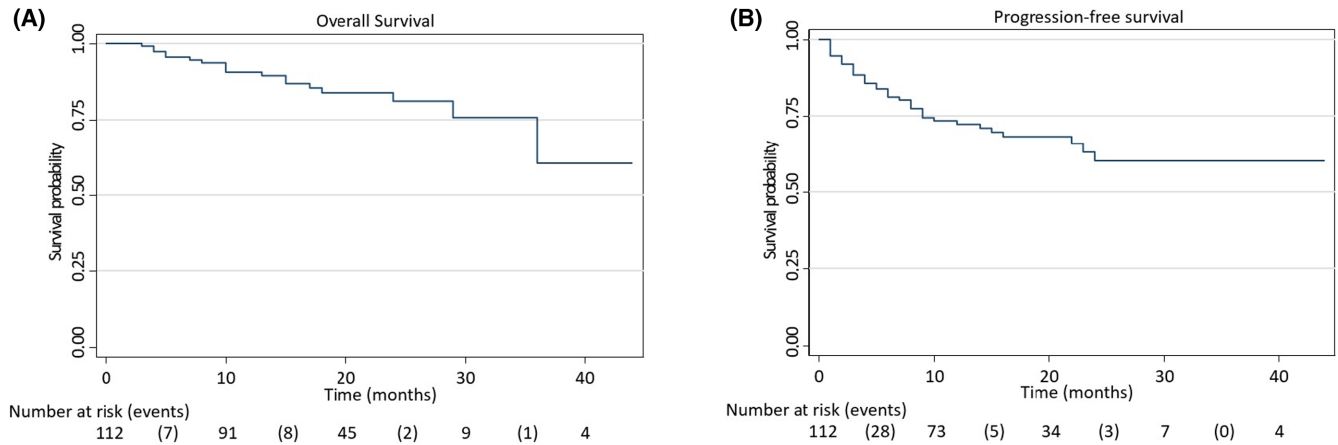


**FIGURE 2** Overall survival (A) and progression-free survival (B) for the whole cohort.

**TABLE 2** Univariate and multivariate analyses for progression-free survival.

Characteristic	Univariate analysis Crude HR [95% CI]	$p^a$	Multivariate analysis adjusted HR [95% CI] $n = 102$	$p^b$
TMTV ( $n = 102$ )				
≤200 mL	1 (ref)	0.002	1 (ref)	0.175
>200 mL	4.58 [1.59–13.15]		2.23 [0.70–7.12]	
ctDNA				
≤3.57 log hGE/mL	1 (ref)	<0.001	1 (ref)	0.385
>3.57 log hGE/mL	3.11 [1.60–6.06]		1.41 [0.65–3.07]	
IPI				
0–2	1 (ref)	<0.001	1 (ref)	0.015
3–5	6.63 [2.57–17.08]		4.04 [1.31–12.41]	
Histological diagnosis				
Other subtypes <sup>c</sup>	1 (ref)	<0.001	1 (ref)	0.003
HGBL	3.96 [1.95–8.02]		3.27 [1.50–7.14]	

Abbreviations: ctDNA, circulating tumoral DNA; HGBL, high grade B-cell lymphoma; IPI, International Prognostic Index; TMTV, total metabolic tumour volume.

<sup>a</sup>Log-rank test.

<sup>b</sup>Multivariable Cox model.

<sup>c</sup>Other subtypes: PMBL and DLBCL.

different prognoses for PFS. Patients with both values above the thresholds ( $n = 28$ ) had a lower 1-year PFS than those with discrepant values ( $n = 41$ ; ctDNA low and TMTV high) or with both values below the thresholds ( $n = 33$ ). One-year PFS estimates for the three groups were 44%, 78% and 97%, respectively ( $p < 0.001$ ; Figure 6).

In the multivariate Cox analysis, only the IPI and the histologic subtype remained significant for predicting PFS ( $p = 0.0015$  and  $p = 0.003$ , respectively; Table 2). Similar results were obtained using a model in which TMTV and ctDNA were considered as a combined variable (low-low/discrepant/high-high), with only IPI and histology remaining significant ( $p = 0.160$  for the combined variable).

## DISCUSSION

This monocentric real-world study reports the combined prognostic value of baseline TMTV and ctDNA load in a cohort of newly diagnosed LBCL patients. A high ctDNA load or a high TMTV at diagnosis were associated with significantly poorer outcome. Correlations between ctDNA load and TMTV have been reported in a few studies, mostly retrospective.<sup>29,33,34,45</sup> To our knowledge, none of these studies assessed their combined prognostic value. Here, we showed that the combination of these two factors highlighted three prognostic groups.

Our study was conducted in a real-world setting with a large cohort of patients. As expected, LBCL subtype distribution and clinical characteristics, including PFS, OS and

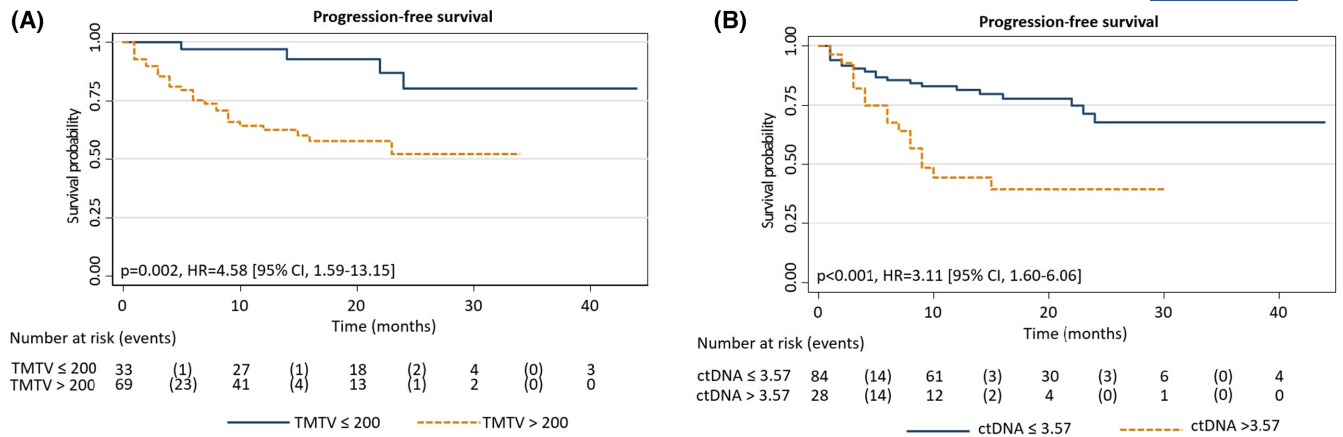


**FIGURE 3** Kaplan–Meier estimates of progression-free survival according to baseline TMTV (A) or baseline ctDNA status (B).

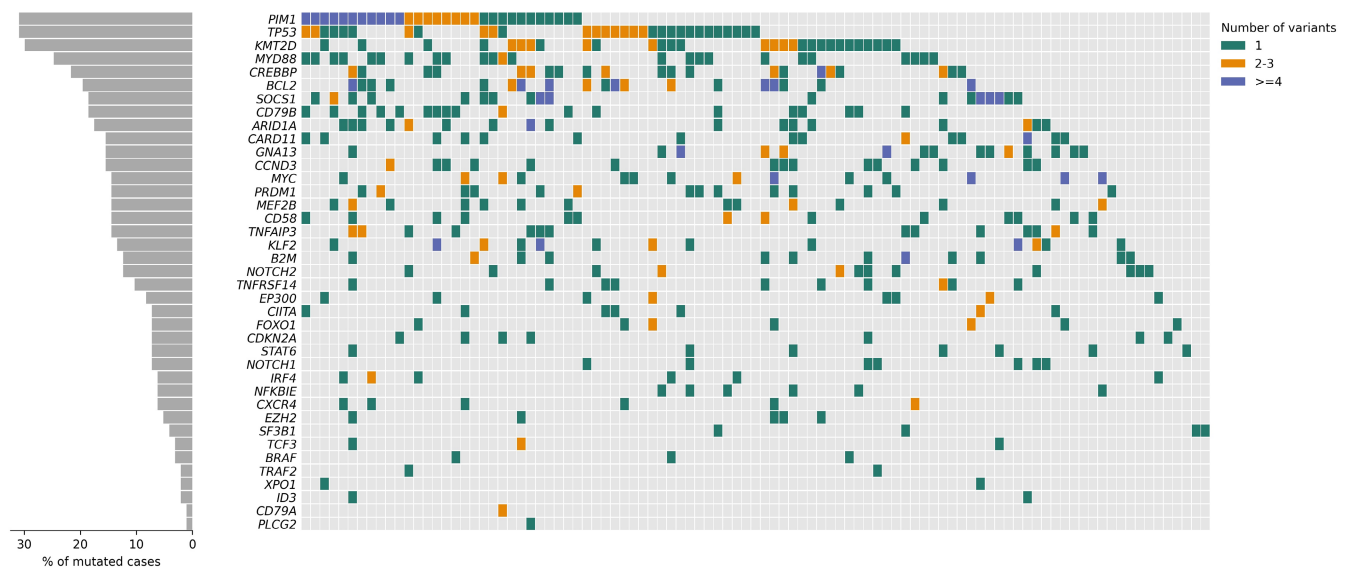


**FIGURE 4** Mutational landscape based on ctDNA analysis. Colours indicate the number of variants (green: 1, yellow: 2–3, blue ≥4).

IPI scores, were in accordance with those observed in previously published studies.<sup>4</sup>

Interest in liquid biopsies is growing. Indeed, liquid biopsies allow the determination of two prognostic parameters: the tumour genetic profile and the quantity of tumoral DNA. In our cohort, ctDNA mutations were detected in 85% of patients. Different rates have been found in previous studies: 63% for Bohers et al.,<sup>29</sup> 66% for Rossi et al.,<sup>28</sup> 87% for Rivas-Delgado,<sup>35</sup> and 98% for Kurtz et al.<sup>33</sup> These differences may be explained by the use of different gene panels. In the current study, we used a lymphopanel designed in 2015 for the purpose of diagnosis, prognosis or theragnosis of B-cell lymphoma.<sup>41</sup> This strategy was similar to that described by Rivas-Delgado et al.<sup>35</sup> and gave similar results. This panel did not include some of the genes used in the most recent DLBCL classifications (such as those described in ref.<sup>46,47</sup>). Nevertheless, it allowed the detection of *TP53* mutations, one of the major prognostic genetic factors identified. Our

results suggested once again the value of this gene in routine prognostic evaluations.

The median ctDNA load reported in our study (2.9 log hGE/mL) was similar to that reported previously.<sup>33,35</sup> As noted in previous studies,<sup>30,31,33–35</sup> a higher pretreatment ctDNA load was prognostic for PFS. No universal cut-off has been defined for ctDNA load. Our threshold of 3.57 log hGE/mL was determined as the optimal cut-off for distinguishing between high- and low-risk patients. This cut-off was significantly higher than those previously reported,<sup>33</sup> which is probably explained in part, by our short follow up.

TMTV is a well-established strong prognostic factor for lymphoma. Our optimal TMTV cut-off was estimated at 200 mL, which was relatively low compared to that used in other studies. TMTV was considered as high when >220 mL in the study by Vercellino et al.,<sup>26</sup> >300 mL in that by Cottreau et al.<sup>15</sup> or >550 mL in the study by Sasanelli et al.<sup>25</sup> To date, several different calculation methods have been proposed



**TABLE 3** Patient characteristics stratified according to pretreatment ctDNA load with the 3.57 log hGE/mL cutoff.

Characteristics	ctDNA ≤3.57 log hGE/mL (n=84)	ctDNA >3.57 log hGE/mL (n=28)	p
Male sex, n (%)	54 (64)	14 (50)	0.18 <sup>b</sup>
Age (years), median [IQR]	65 [53.5–73.5]	71 [55–77]	0.094 <sup>c</sup>
Histological diagnosis, n (%)			
DLBCL	66 (79)	21 (75)	0.228 <sup>d</sup>
HGBL	10 (12)	7 (25)	
PMBL	5 (6)	0 (0)	
Other <sup>a</sup>	3 (4)	0 (0)	
Histological diagnosis, n (%)			
Other subtypes	74 (88)	21 (75)	0.127 <sup>d</sup>
HGBL	10 (12)	7 (25)	
Transformed low grade, n (%)	19 (23)	9 (3)	0.313 <sup>b</sup>
Stage, n (%)			
I/II	18 (21)	1 (4)	0.039 <sup>d</sup>
III/IV	66 (79)	27 (96)	
IPI, n (%)			
0–2	48 (57)	3 (11)	<0.001 <sup>b</sup>
3–5	36 (43)	25 (89)	
CNS-IPI, n (%)			
0–1	22 (26)	0 (0)	<0.001 <sup>b</sup>
2–3	47 (56)	8 (29)	
4–6	15 (18)	20 (71)	
LDH above normal, n (%)	39 (46)	28 (100)	<0.001 <sup>b</sup>
Central nervous system localization <sup>e</sup> , n (%)	5 (6)	0 (0)	0.330 <sup>d</sup>
Bone marrow involvement <sup>f</sup> , n (%)	7 (9)	7 (29)	0.019 <sup>d</sup>
Histological features, n (%)			
GC	48 (57)	6 (21)	0.001 <sup>b</sup>
Non-GC	36 (43)	22 (79)	

Abbreviations: CNS-IPI, Central Nervous system-International Prognostic Index; DLBCL, diffuse large B-cell lymphoma; FDG-PET/CT, <sup>18</sup>F-fluorodeoxyglucose -positron emission tomography/computed tomography; GC, Germinal Center (according to Hans algorithm); HGBL, high grade B-cell lymphoma; IPI, International Prognostic Index; LDH, lactate dehydrogenase level; PMBL, primary mediastinal large B-cell lymphoma; TMTV, total metabolic tumour volume.

<sup>a</sup>Two patients had T-cell-rich B-cell lymphoma and one had intravascular DLBCL.

<sup>b</sup>Chi-squared test.

<sup>c</sup>Student's *t* test.

<sup>d</sup>Fisher test.

<sup>e</sup>n = 82 for the ctDNA ≤3.57 log hGE/mL group and n = 27 for the ctDNA >3.57 log hGE/mL group.

<sup>f</sup>n = 78 for the ctDNA ≤3.57 log hGE/mL group and n = 24 for the ctDNA >3.57 log hGE/mL group.

and could explain these differences.<sup>48</sup> However, irrespective of methodology, TMTV remains a robust prognostic parameter in DLBCL.<sup>15,22,25,26,35,48</sup> In our study, TMTV was calculated using a fully automated artificial intelligence-based method for the segmentation of lymphoma lesions.<sup>39</sup> Volume quantification and lymphoma segmentation are key to ensuring reliable measurement of TMTV. Fully automatic segmentation has been shown to improve the reproducibility of TMTV assessments. As proposed by Barrington and Meignan,<sup>48</sup> standardization will improve the use of this parameter in clinical practice.

Associations between TMTV and other prognostic factors<sup>15,26</sup> have been studied and allowed a better stratification of LBCL patients. The combination of baseline TMTV and

ctDNA load, reported here, stratified the population into three different groups prognostic for PFS and provided a strong predictor of early disease events. Patients with both values below the thresholds had a significantly better PFS than the other groups. The fact that all the patients with discordant values presented high TMTV (>200 mL) was unexpected. Moreover, these patients had a better 1-year PFS than those with both values above the thresholds. Our findings suggest that ctDNA, as a good indicator of tumour mass and aggressiveness, provides additional information for estimating LBCL prognosis, mitigating the strong impact of TMTV. Thus, our results enabled, in a short follow-up time, the identification of patients with a very good prognosis (TMTV ≤200 mL) and the identification of patients

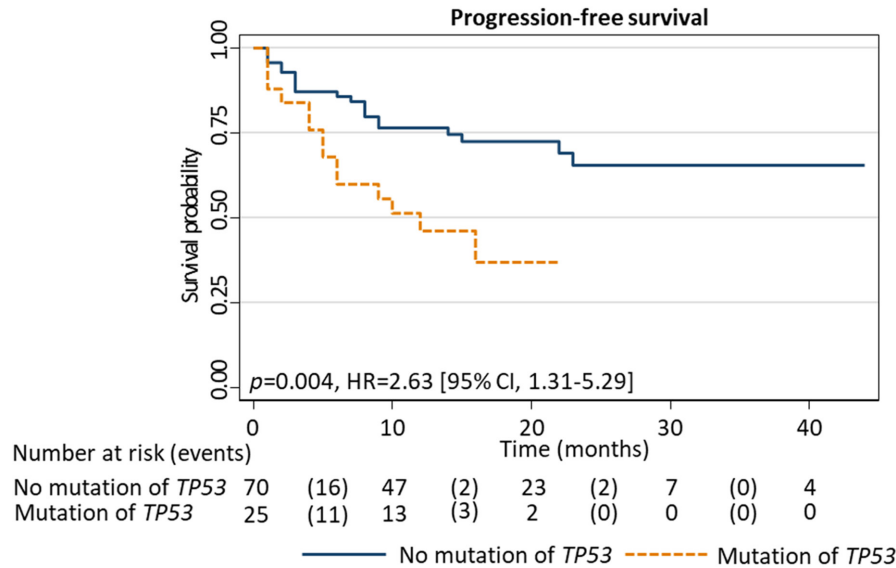


**FIGURE 5** Kaplan–Meier estimates of progression-free survival according to *TP53* mutation status (ctDNA >0 log hGE/mL).

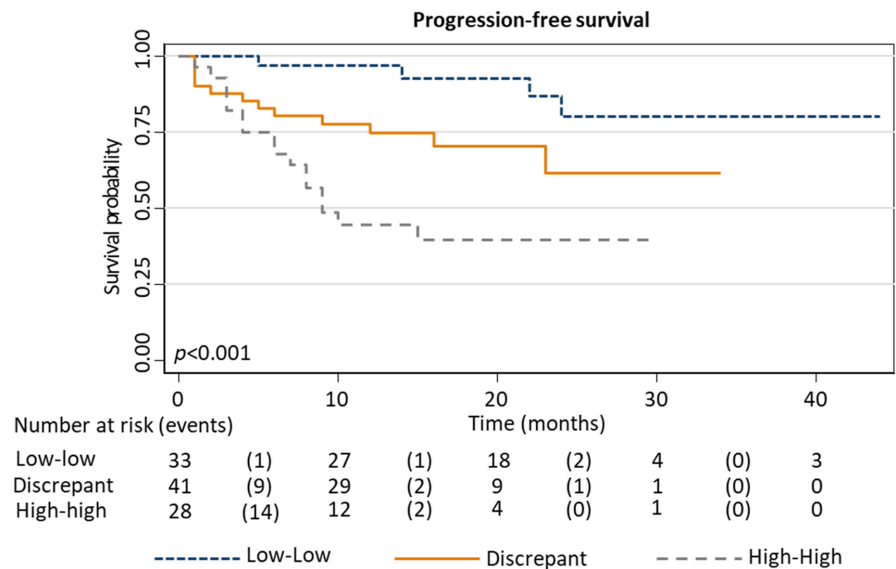


**FIGURE 6** Kaplan–Meier estimates of progression-free survival according to ctDNA load at diagnosis with baseline TMTV.

with a very high risk of early relapse (TMTV >200 mL and ctDNA >3.57 log hGE/mL). Further studies involving larger cohorts are needed to confirm these findings, and to develop and evaluate the potential use of a prognostic score including ctDNA, TMTV, IPI and *TP53* mutations.

The non-significance of ctDNA in the multivariate analysis results were unexpected and contradicts the findings of previous studies.<sup>33</sup> This may be explained by our short follow-up period, which limited the number of disease events. Studies with a longer follow-up period are required.

In conclusion, combining ctDNA load with TMTV at diagnosis improved the risk stratification of patients with aggressive B-cell lymphoma and appeared to be strong

predictor of early disease events, allowing better and earlier identification of very high-risk patients, who could benefit from the rapid introduction of new therapies, like CAR T-cell therapy or bispecific antibodies.

#### AUTHOR CONTRIBUTIONS

E.L.G. contributed to the data collection and wrote the paper. M.H.D.L., C.H., L.R., F.L. contributed to the study design and supervision, analyzed and provided the data. P.G., E.I. and P.B.D. provided the data and edited the manuscript. C.C.B., E.P., C.R. provided and analyzed the data. G.G., A.A., I.B., A.C. and D.L.M.B. analyzed the data. C.L. and E.I. performed statistical analyses.

## ACKNOWLEDGEMENTS

We would like to thank all the clinicians of the lymphoid haemopathy unit and the technicians of the immunology laboratory without whom this work could not have been carried out.

## FUNDING INFORMATION

We thank Roche and Celgene for their support of the ARTGIL association (Association for Therapeutic, Genetic and Immunological research on Lymphoma).

## CONFLICT OF INTEREST STATEMENT

Marie-Helene Delfau-Larue received funding for travel/accommodation from Baxter, Janssen, and Celgene. Corinne Haioun had a consulting role for Roche and received research funding from Roche and Amgen. Philippe Gaulard had a consulting role for Takeda and Gilead and received research grants from Innate Pharma, Takeda and Sanofi. Louis Roulin had a consulting role for Gilead. The other authors declare that they have no conflicts of interest.

## DATA AVAILABILITY STATEMENT


The data that support the findings of this study (NGS DATA) are openly available in supplementary data.

## PATIENT CONSENT STATEMENT

All patients provided written informed consent before being included in the analysis for the current study, in accordance with both institutional ethical guidelines and the Declaration of Helsinki.

## ORCID

Enora Le Goff  <https://orcid.org/0000-0003-1724-3909>

Marie-Helene Delfau-Larue  <https://orcid.org/0000-0002-8010-2343>

## REFERENCES

- Alaggio R, Amador C, Anagnostopoulos I, Attygalle AD, Araujo IBO, Berti E, et al. The 5th edition of the World Health Organization classification of Haematolymphoid Tumours: lymphoid neoplasms. *Leukemia* 2022;22:1–29.
- Swerdlow SH, Campo E, Pileri SA, Harris NL, Stein H, Siebert R, et al. The 2016 revision of the World Health Organization classification of lymphoid neoplasms. *Blood*. 2016;127(20):2375–90.
- Coiffier B, Thieblemont C, Van Den Neste E, Lepeu G, Plantier I, Castaigne S, et al. Long-term outcome of patients in the LNH-98.5 trial, the first randomized study comparing rituximab-CHOP to standard CHOP chemotherapy in DLBCL patients: a study by the Groupe d'Etudes des Lymphomes de l'Adulte. *Blood*. 2010;116(12):2040–5.
- Sehn LH, Salles G. Diffuse Large B-Cell Lymphoma. *N Engl J Med*. 2021;384(9):842–58.
- Crump M, Neelapu SS, Farooq U, Van Den Neste E, Kuruvilla J, Westin J, et al. Outcomes in refractory diffuse large B-cell lymphoma: results from the international SCHOLAR-1 study. *Blood*. 2017;130(16):1800–8.
- International Non-Hodgkin's Lymphoma Prognostic Factors Project. A predictive model for aggressive non-Hodgkin's lymphoma. *N Engl J Med*. 1993;329(14):987–94.
- Sehn LH, Berry B, Chhanabhai M, Fitzgerald C, Gill K, Hoskins P, et al. The revised International Prognostic Index (R-IPI) is a better predictor of outcome than the standard IPI for patients with diffuse large B-cell lymphoma treated with R-CHOP. *Blood*. 2007;109(5):1857–61.
- Zhou Z, Sehn LH, Rademaker AW, Gordon LI, LaCasce AS, Crosby-Thompson A, et al. An enhanced international prognostic index (NCCN-IPI) for patients with diffuse large B-cell lymphoma treated in the rituximab era. *Blood*. 2014;123(6):837–42.
- Schmitz N, Zeynalova S, Nickelsen M, Kansara R, Villa D, Sehn LH, et al. CNS international prognostic index: a risk model for CNS relapse in patients with diffuse large B-cell lymphoma treated with R-CHOP. *J Clin Oncol*. 2016;34(26):3150–6.
- Dubois S, Viailly PJ, Mareschal S, Bohers E, Bertrand P, Ruminy P, et al. Next-generation sequencing in diffuse large B-cell lymphoma highlights molecular divergence and therapeutic opportunities: a LYSA study. *Clin Cancer Res*. 2016;22(12):2919–28.
- Alizadeh AA, Eisen MB, Davis RE, Ma C, Lossos IS, Rosenwald A, et al. Distinct types of diffuse large B-cell lymphoma identified by gene expression profiling. *Nature*. 2000;403(6769):503–11.
- Rosenwald A, Wright G, Chan WC, Connors JM, Campo E, Fisher RI, et al. The use of molecular profiling to predict survival after chemotherapy for diffuse large-B-cell lymphoma. *N Engl J Med*. 2002;346(25):1937–47.
- Scott DW, Mottok A, Ennishi D, Wright GW, Farinha P, Ben-Neriah S, et al. Prognostic significance of diffuse large B-cell lymphoma cell of origin determined by digital gene expression in formalin-fixed paraffin-embedded tissue biopsies. *J Clin Oncol*. 2015;33(26):2848–56.
- Lenz G, Wright G, Dave SS, Xiao W, Powell J, Zhao H, et al. Stromal gene signatures in large-B-cell lymphomas. *N Engl J Med*. 2008;359(22):2313–23.
- Cottreau AS, Lanic H, Mareschal S, Meignan M, Vera P, Tilly H, et al. Molecular profile and FDG-PET/CT Total metabolic tumor volume improve risk classification at diagnosis for patients with diffuse large B-cell lymphoma. *Clin Cancer Res*. 2016;22(15):3801–9.
- Staiger AM, Ziepert M, Horn H, Scott DW, Barth TFE, Bernd HW, et al. Clinical impact of the cell-of-origin classification and the MYC/BCL2 dual expresser status in diffuse large B-cell lymphoma treated within prospective clinical trials of the German high-grade non-Hodgkin's lymphoma study group. *J Clin Oncol*. 2017;35(22):2515–26.
- Scott DW, King RL, Staiger AM, Ben-Neriah S, Jiang A, Horn H, et al. High-grade B-cell lymphoma with MYC and BCL2 and/or BCL6 rearrangements with diffuse large B-cell lymphoma morphology. *Blood*. 2018;131(18):2060–4.
- Savage KJ, Johnson NA, Ben-Neriah S, Connors JM, Sehn LH, Farinha P, et al. MYC gene rearrangements are associated with a poor prognosis in diffuse large B-cell lymphoma patients treated with R-CHOP chemotherapy. *Blood*. 2009;114(17):3533–7.
- Rosenwald A, Bens S, Advani R, Barrans S, Copie-Bergman C, Elsensohn MH, et al. Prognostic significance of MYC rearrangement and translocation partner in diffuse large B-cell lymphoma: a study by the Lunenburg lymphoma biomarker consortium. *J Clin Oncol*. 2019;37(35):3359–68.
- Copie-Bergman C, Cuillière-Dartigues P, Baia M, Briere J, Delarue R, Canioni D, et al. MYC-IG rearrangements are negative predictors of survival in DLBCL patients treated with immunochemotherapy: a GELA/LYSA study. *Blood*. 2015;126(22):2466–74.
- Barrington SF, Mikhael NG, Kostakoglu L, Meignan M, Hutchings M, Müller SP, et al. Role of imaging in the staging and response assessment of lymphoma: consensus of the International Conference on Malignant Lymphomas Imaging Working Group. *JCO*. 2014;32(27):3048–58.
- Meignan M, Itti E, Gallamini A, Younes A. FDG PET/CT imaging as a biomarker in lymphoma. *Eur J Nucl Med Mol Imaging*. 2015;42(4):623–33.
- Cheson BD, Fisher RI, Barrington SF, Cavalli F, Schwartz LH, Zucca E, et al. Recommendations for initial evaluation, staging, and

- response assessment of Hodgkin and non-Hodgkin lymphoma: the Lugano classification. *J Clin Oncol.* 2014;32(27):3059–68.
24. Meignan M, Sasanelli M, Casasnovas RO, Luminari S, Fioroni F, Coriani C, et al. Metabolic tumour volumes measured at staging in lymphoma: methodological evaluation on phantom experiments and patients. *Eur J Nucl Med Mol Imaging.* 2014;41(6):1113–22.
  25. Sasanelli M, Meignan M, Haioun C, Berriolo-Riedinger A, Casasnovas RO, Biggi A, et al. Pretherapy metabolic tumour volume is an independent predictor of outcome in patients with diffuse large B-cell lymphoma. *Eur J Nucl Med Mol Imaging.* 2014;41(11):2017–22.
  26. Vercellino L, Cottreau AS, Casasnovas O, Tilly H, Feugier P, Chartier L, et al. High total metabolic tumor volume at baseline predicts survival independent of response to therapy. *Blood.* 2020;135(16):1396–405.
  27. Diaz LA, Bardelli A. Liquid biopsies: genotyping circulating tumor DNA. *J Clin Oncol.* 2014;32(6):579–86.
  28. Rossi D, Diop F, Spaccarotella E, Monti S, Zanni M, Rasi S, et al. Diffuse large B-cell lymphoma genotyping on the liquid biopsy. *Blood.* 2017;129(14):1947–57.
  29. Bohers E, Viailly PJ, Becker S, Marchand V, Ruminy P, Maingonnat C, et al. Non-invasive monitoring of diffuse large B-cell lymphoma by cell-free DNA high-throughput targeted sequencing: analysis of a prospective cohort. *Blood Cancer J.* 2018;8(8):1–13.
  30. Roschewski M, Staudt LM, Wilson WH. Dynamic monitoring of circulating tumor DNA in non-Hodgkin lymphoma. *Blood.* 2016;127(25):3127–32.
  31. Hohaus S, Giachelia M, Massini G, Mansueto G, Vannata B, Bozzoli V, et al. Cell-free circulating DNA in Hodgkin's and non-Hodgkin's lymphomas. *Ann Oncol.* 2009;20(8):1408–13.
  32. Roschewski M, Dunleavy K, Pittaluga S, Moorhead M, Pepin F, Kong K, et al. Comparative study of circulating tumor DNA and computerized tomography monitoring in untreated diffuse large B-cell lymphoma. *Lancet Oncol.* 2015;16(5):541–9.
  33. Kurtz DM, Scherer F, Jin MC, Soo J, Craig AFM, Esfahani MS, et al. Circulating tumor DNA measurements As early outcome predictors in diffuse large B-cell lymphoma. *JCO.* 2018;36(28):2845–53.
  34. Scherer F, Kurtz DM, Newman AM, Stehr H, Craig AFM, Esfahani MS, et al. Distinct biological subtypes and patterns of genome evolution in lymphoma revealed by circulating tumor DNA. *Sci Transl Med.* 2016;8(364):364ra155.
  35. Rivas-Delgado A, Nadeu F, Enjuanes A, Casanueva-Eliceiry S, Mozas P, Magnano L, et al. Mutational landscape and tumor burden assessed by cell-free DNA in diffuse large B-cell lymphoma in a population-based study. *Clin Cancer Res.* 2021;27(2):513–21.
  36. Copie Bergman C, Bohers E, Dartigues-Cuillères P, Viailly PJ, Ruminy P, Marchand V, et al. Real time pathological and molecular characterization of aggressive B-cell lymphomas based on a National Network. A Lysa project. *Blood.* 2020;5(136):22–3.
  37. Delfau-Larue MH, van der Gucht A, Dupuis J, Jais JP, Nel I, Beldi-Ferchiou A, et al. Total metabolic tumor volume, circulating tumor cells, cell-free DNA: distinct prognostic value in follicular lymphoma. *Blood Adv.* 2018;2(7):807–16.
  38. Meignan M, Gallamini A, Meignan M, Gallamini A, Haioun C. Report on the first international workshop on interim-PET-scan in lymphoma. *Leuk Lymphoma.* 2009;50(8):1257–60.
  39. Blanc-Durand P, Jégou S, Kanoun S, Berriolo-Riedinger A, Bodet-Milin C, Kraeber-Bodéré F, et al. Fully automatic segmentation of diffuse large B cell lymphoma lesions on 3D FDG-PET/CT for total metabolic tumour volume prediction using a convolutional neural network. *Eur J Nucl Med Mol Imaging.* 2021;48(5):1362–70.
  40. Hans CP, Weisenburger DD, Greiner TC, Gascoyne RD, Delabie J, Ott G, et al. Confirmation of the molecular classification of diffuse large B-cell lymphoma by immunohistochemistry using a tissue microarray. *Blood.* 2004;103(1):275–82.
  41. Bohers E, Viailly PJ, Dubois S, Bertrand P, Maingonnat C, Mareschal S, et al. Somatic mutations of cell-free circulating DNA detected by next-generation sequencing reflect the genetic changes in both germinal center B-cell-like and activated B-cell-like diffuse large B-cell lymphomas at the time of diagnosis. *Haematologica.* 2015;100(7):e280–4.
  42. Camp RL, Dolled-Filhart M, Rimm DL. X-tile: a new bio-informatics tool for biomarker assessment and outcome-based cut-point optimization. *Clin Cancer Res.* 2004;10(21):7252–9.
  43. Rosenberg SA. Validity of the Ann Arbor staging classification for the non-Hodgkin's lymphomas. *Cancer Treat Rep.* 1977;61(6):1023–7.
  44. Ribrag V, Koscielny S, Bosq J, Leguay T, Casasnovas O, Fornecker LM, et al. Rituximab and dose-dense chemotherapy for adults with Burkitt's lymphoma: a randomised, controlled, open-label, phase 3 trial. *Lancet.* 2016;387(10036):2402–11.
  45. Kurtz DM, Green MR, Bratman SV, Scherer F, Liu CL, Kunder CA, et al. Noninvasive monitoring of diffuse large B-cell lymphoma by immunoglobulin high-throughput sequencing. *Blood.* 2015;125(24):3679–87.
  46. Wright GW, Huang DW, Phelan JD, Coulibaly ZA, Roulland S, Young RM, et al. A probabilistic classification tool for genetic subtypes of diffuse large B cell lymphoma with therapeutic implications. *Cancer Cell.* 2020;37(4):551–568.e14.
  47. Chapuy B, Stewart C, Dunford AJ, Kim J, Kamburov A, Redd RA, et al. Molecular subtypes of diffuse large B cell lymphoma are associated with distinct pathogenic mechanisms and outcomes. *Nat Med.* 2018;24(5):679–90.
  48. Barrington SF, Meignan M. Time to prepare for risk adaptation in lymphoma by standardizing measurement of metabolic tumor burden. *J Nucl Med.* 2019;60(8):1096–102.

## SUPPORTING INFORMATION

Additional supporting information can be found online in the Supporting Information section at the end of this article.

**How to cite this article:** Le Goff E, Blanc-Durand P, Roulin L, Lafont C, Loyaux R, MBoumbae D-L, et al. Baseline circulating tumour DNA and total metabolic tumour volume as early outcome predictors in aggressive large B-cell lymphoma. A real-world 112-patient cohort. *Br J Haematol.* 2023;00:1–11. <https://doi.org/10.1111/bjh.18809>